ESTIMATION OF ABOVE GROUND FOREST BIOMASS IN A TIGER HABITAT OF THE WESTERN NEPAL USING ALOS DATA AND FIELD INVENTORY

*S. Nashrrullah[a], S. Khanal[b], G.J. Thapa[c], M.K. Hazarika[a] and L. Samarakoon[a]

[a] Geoinformatics Center, Asian Institute of Technology
P.O. Box 4, Klong Luang, Pathumthani 12120, Thailand; Tel: +66-2-524-5580; E-mail: syams@ait.asia

[b] Department of Forest Research and Survey, Nepal
E-mail: shiva_kanal@yahoo.com

[c] World Wildlife Fund for Nature, Nepal
E-mail: gokarna.thapa@wwfnepal.org

KEY WORDS: ALOS/PALSAR, above ground biomass, multi-temporal radar imageries, radar backscatter, forest inventory, western Nepal

Abstract: This study aims to apply remote sensing approach for estimating above ground forest biomass of the Western Tiger Landscape of Nepal. Multi-temporal radar imageries of L-band ALOS/PALSAR were used to provide data of radar backscatter coefficients. In-situ data of above ground forest biomass was calculated from the field inventory data using an allometric equation. In total, there were 14 ALOS/PALSAR scenes and 358 forest plots which were analyzed to meet the objectives. The relationships between radar backscatter coefficient and in-situ above ground forest biomass were analyzed over a grid with cell size of 9 by 9 pixels (approximately 1 hectare). Then, a non-linier regression approach was used to develop a biomass model. Finally, the best-fit biomass model was applied to produce biomass map of the study area.

In comparison between the radar backscatter of mono- and multi-temporal L-band ALOS/PALSAR imageries, the multi-temporal data generally shows a better correlation with the above ground forest biomass calculated from field data. The multi-temporal approach compensates variable climatic conditions of a single radar image. The biomass model which developed using a non-linier regression analysis successfully produced biomass map. However, the accuracy should be improve and like other similar research that utilize radar backscatter coefficient to estimate biomass, use of L-band also has a constraint in terms of biomass saturation (around 100-150 t/ha). Although, the saturation level for L-band is quite high (>100 t/ha) compared to the reported values for X- and C-band (30-50 t/ha).

INTRODUCTION

Global concerns on issues related to climate change and global warming have also increased interest in the role of forests in reducing greenhouse gasses emissions. Forests are known as the major carbon sinks that approximately account for 72% of the earth's terrestrial carbon storage and absorb one twelfth of the atmospheric carbon dioxide stock every year (Ghasemi et al., 2010). An international initiative on "Reducing Emissions from Deforestation and forest Degradation and the role of conservation, sustainable management of forests and enhancement of forest carbon stocks in developing countries" (REDD+) provides an opportunity for a developing country like Nepal, of not only mitigate the climate change, but can also support livelihood and preserve the biodiversity of forest ecosystems. Accurate measurements of biomass and carbon stocks and the subsequent monitoring of the forest carbon pool are essential requirements for a successful implementation of REDD+ (Asner, 2009; Gibbs et al., 2007).

Biomass is defined as mass of live or dead organic matter that includes the above-ground and below-ground living biomass, dead mass, and litter (GTOS, 2009). The largest carbon pool are typically stored in the aboveground living biomass, thus, estimating aboveground forest biomass (AGB) is the most important step in quantifying carbon stocks from forests (Gibbs et al., 2007). The most accurate ways of calculating biomass data is based on field measurement through destructive sampling or allometric equations method (Englhart et al., 2011, Lu, 2006). However, these methods are often cost and time consuming, labor intensive, have limited spatial distribution, and impractical especially in remote areas (Englhart et al., 2011; Gibbs et al., 2007; Lu, 2006). Remote sensing techniques have the capacity to overcome the limitations of conventional field measurement methods and have now become the primary source in estimating AGB (Lu, 2006; Patenaude et al., 2005).

The acquisition of high quality remote sensing data by optical sensors are often hampered by the frequent cloud covers. In such conditions, microwave remote sensing or radar is the only feasible source of remotely sensed data because of their advantages in weather and daylight independency (Lu, 2006). The land cover and terrain properties such as surface roughness and moisture content, as well as the properties of radar sensor such as wavelength, polarization, and incidence angle influence the radar capability on biomass estimation (Englhart et al., 2011). A number of studies have shown that the radar backscatter in the longer wavelengths (L- or P-bands) is more highly correlated with the forest parameters such as tree age, tree height, DBH, basal area, and AGB compare to the shorter wavelengths (C-band) (Lu, 2006). The use of L-band of ALOS/PALSAR data for calculating biomass have been investigated by many researchers using different approaches (Englhart et al., 2011; Lucas et al., 2010; Mitchard et al., 2011; Morel et al., 2011; Sarker et al., 2012; Sun et al., 2011). This study aims to investigate the use of multi-temporal and dual polarizations of ALOS/PALSAR data in estimating forest biomass in the Western Terain Landscape of Nepal.

STUDY AREA

The study site is situated in the most western Terai Landcape of Nepal, particularly Kailali and Kanchanpur districts. The area stretches from lowland of Terai in the south and touches a bit portion of Siwalik region in the northern part, with elevation varies within south-north segment from 130 to 1900m above the sea level. Climate varies from tropical to sub-tropical depending upon the geographical variation. This area covers part of the conservation area of Nepal, which were established in order to preserve the biodiversity, forests, soil, and watersheds of the Terai and Churia Hills. Furthermore, it is home to the coexistence of the few remaining habitats of three endangered large mammals (Tigers, Elephants and Rhinos) as well as many other important flora and faunas (Gurung and Kokh, 2011).

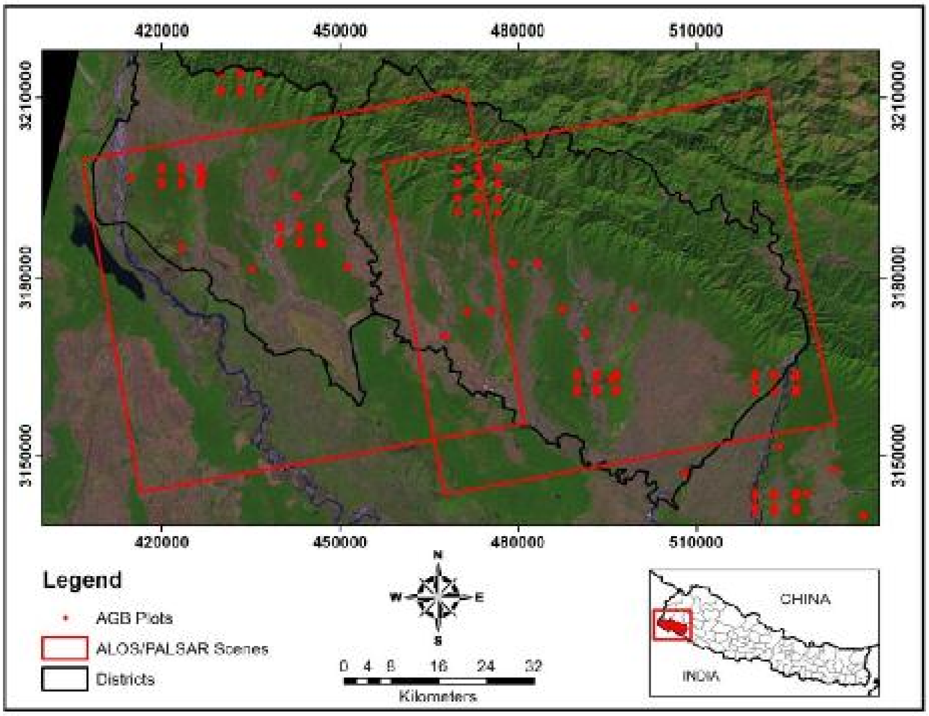

Figure 1: Location of the study area overlay with the ground plots and ALOS/PALSAR scene outlines.

DATASETS

Forest field inventory data were collected from the Forest Resource Assessment (FRA), Nepal. The data were measured during field campaign in 2010-2011, as part of the bilateral co-operation project between Governments of Nepal and Finland (http://franepal.org/index.php). In total 358 plots were measured, consist of plots in agricultural area (Ag), several forest type including Sal - Shorea robusta (S), Acacia catechu and Dalbergia sisso (KS/SK), Tropical mixed hardwoods (TMH), Lower mixed hardwood (LMH), and Pinus roxburghii (Pr), and others (SB). Trees within a circular plot of 20m radius were measured and structural parameters including tree height, diameter at breast height (DBH), and tree species were collected in order to calculate the above ground biomass (AGB) using allometric equations. The calculation procedure produced a plot-wise AGB in tons per hectare. Overall number of plots was 358 plots located in both scenes.

In order to cover the whole study area, multi-temporal of ALOS/PALSAR data from two scenes between 2007 and 2010 were collected from JAXA, with a total of 8 images from scene 518-560 and 6 images from scene 519-560. All data were acquired in fine beam dual mode (HH and HV polarization) at off-nadir angle of 34.3° and delivered in Level 1.5 processing level as a geocode multi-look image with a pixel spacing of 12.5m.

METHODS

The ALOS/PALSAR data were processed in order to derive backscatter coefficient in decibel values. The following processing steps were carried out including terrain correction, co-registration, radiometric calibration and adaptive filtering. With the use of 90m resolution of DEM (Digital Elevation Model) from SRTM (Shuttle Radar Topography Mission), terrain correction was done in ASF MapReady software to reduce effects of illuminated target area caused by topography and SAR image geometry. For multi-temporal processing and analysis, co-registration was performed in order to align the images on pixel level and remove shifts between images on different dates. Radiometric calibration was applied for all scenes using the following equation:

$$\sigma°[dB] = 10\log_{10}(DN)^2 + CF \qquad (1)$$

where σ° is the backscatter coefficient, DN is the digital number of image pixel, and CF is the calibration factor set at -83 (Shimada et al., 2009). The images were then filtered using Lee filter with 3 by 3 pixels window size to reduce speckle in the images. For multi-temporal approach, single images of each scene were averaged and analyzed in yearly and whole time span basis.

The relationships between the resulted radar backscatter values and the AGB values from field measurement were analyzed over a grid with a cell size of 9 by 9 pixels (approximately 1 hectare), to match the scale of the regression model. Then, a non-linier regression approach was used to develop a biomass model. Finally, a biomass map of the study area was produced using the best-fit biomass model.

RESULTS & DISCUSSIONS

Above ground biomass calculated from the forest field inventory data were analyzed for each cover and forest types, and presented in box-plots (Figure 2). The diagram provides visual representation of the data distribution, shows the first quartile, third quartile and median of biomass for each class, and also highlights those values that are greatly differ from the other values or outlier.

The largest number of plots lies in the predominant forest TMH (Tropical Mixed Hardwoods) with 281 plots, followed by Sal forest (49 plots), LMH (14 plots), Pr (7), KS/SK (4 plots), agriculture (2 plots), and others (1 plot). The minimum AGB value is 0.981 tons/ha and maximum is 1835.212 tons/ha, with mean value is 290.781 ton/ha. From Figure 2a, it is clear that AGB in Sal forest is the highest (average of more than 250 tons/ha), followed by TMH, LMH, Pinus roxburghii, Acacia catechu and Dalbergia sisso, Agriculture, and others.

As can be seen from Figure 2a, outliers are clearly viewed at higher biomass especially in TMH forest type. For analysis purpose, AGB with more than 600 tons/ha were excluded in order to remove the outliers and the diagram of the result are visualized in Figure 2b. Due to limited number of plots, only Sal and TMH forest type are considered for further analysis. In the end, the number of plots used for biomass regression modeling was 236 plots, with 123 plots located in each scene.

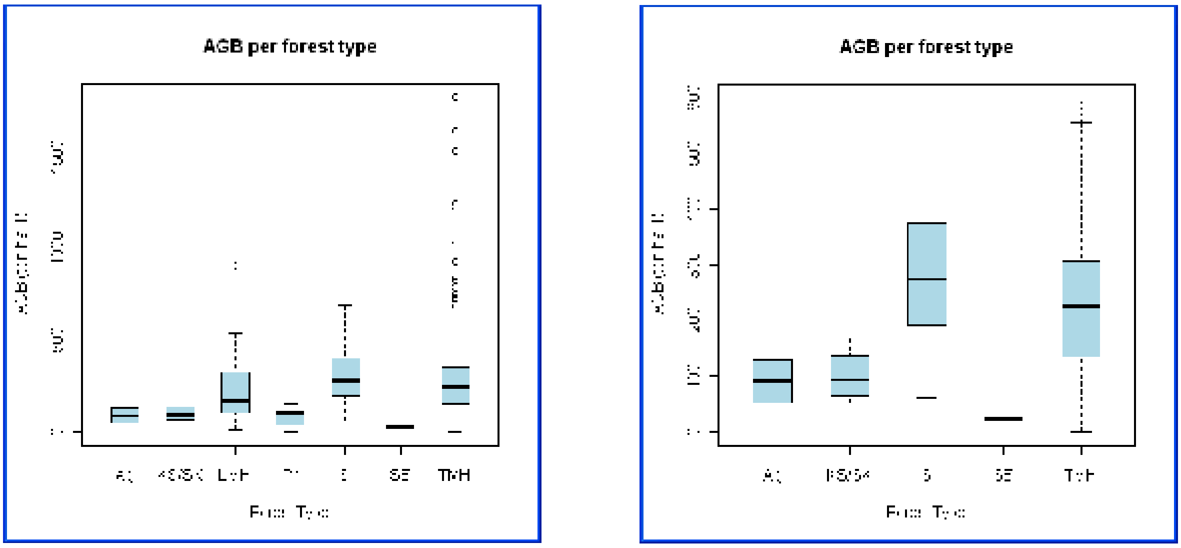

(a) (b)

Figure 2: Box-plot of the AGB calculated from field data with (a) All datasets; (b) Exclusion of plots with AGB more than 600 tons/ha

Pearson's product moment correlation between AGB and backscatter coefficient were calculated to evaluate the correlation strength for different forest type (all classes, Sal, and TMH), polarization (HH and HV), and temporal data (single- and multi-dates). Table 1 and Table 2 shows the value of r and their corresponding p-values for scene 518-560 and 519-560, respectively. When comparing the value of r for different forest types with the value of all classes, in general, there is no improvement in the use of specific forest type (either Sal or TMH). The reason could be that the samples plots were not in sufficient number to analyze forest class separately, especially for Sal forest.

Table 1: Pearson's product moment correlation between AGB and backscatter coefficient for scene 518-560

		Scene 518-560					
		All classes		Sal		TMH	
		HH	HV	HH	HV	HH	HV
15 Jun 2007	r	0.3405	0.3939	0.39187	0.3296	0.24973	0.34167
	p-value	0.0002	2.059e-06	0.2627	0.3522	0.0152	0.00075
15 Sep 2007	r	0.4951	0.4126	0.18189	0.38584	0.45182	0.35794
	p-value	3.825e-08	7.452e-06	0.615	0.2708	4.85e-06	0.00039
2007	r	0.4247	0.4121	0.41671	0.3895	0.3512	0.35592
	p-value	3.747e-06	7.699e-06	0.2309	0.2659	0.00051	0.00043
2 May 2008	r	0.4685	0.4317	0.26877	0.47464	0.42453	0.42141
	p-value	2.437e-07	2.48e-06	0.4527	0.8964	2.004e-05	2.338e-05
2008	r	0.4685	0.4317	0.26877	0.47464	0.42453	0.42141
	p-value	2.437e-07	2.48e-06	0.4527	0.8964	2.004e-05	2.338e-05
20 Jun 2009	r	0.4384	0.3967	0.03875	0.29315	0.42445	0.36194
	p-value	1.66e-06	1.779e-05	0.9153	0.411	2.012e-05	0.00033
5 Aug 2009	r	0.4321	0.36788	0.4565	0.25301	0.37315	0.330107
	p-value	2.431e-06	7.688e-05	0.1847	0.4806	0.00021	0.001157
20 Sep 2009	r	0.4364	0.34517	0.63212	0.9258	0.39635	0.33133
	p-value	1.87e-06	0.00022	0.04986	0.7992	7.667e-05	0.00110
2009	r	0.47130	0.3833	0.4617	0.22703	0.4274	0.36629
	p-value	2.028e-07	3.577e-05	0.1791	0.5282	1.728e-05	0.00028
23 Jun 2010	r	0.3510	0.4142	0.369015	0.41781	0.30535	0.37447
	p-value	0.00016	6.847e-06	0.294	0.2296	0.0027	0.00020
8 Aug 2010	r	0.34663	0.36738	0.16042	0.20822	0.30930	0.34632
	p-value	0.0002	7.876e-05	0.658	0.5637	0.00241	0.00062
2010	r	0.3562	0.3973	0.28730	0.329505	0.3138	0.36629
	p-value	0.0001	1.725e-05	0.4209	0.3525	0.00205	0.00028
2007-2010	r	0.4513	0.4425				
	p-value	7.491e-07	1.3e-06				

A number of studies in biomass estimation using ALOS/PALSAR have concluded that the HV polarization showed higher correlation with AGB compare to the HH polarization (Englhart et al., 2011, Mitchard et al., 2011, Tian et al., 2012). The correlation result for scene 519-560 is having a good agreement with previous mentioned studies, as can be seen in Table 2. However, in case of scene 518-560 (see Table 1), it is found that the correlation strength between HH and HV is not very much different or even slightly less for HV polarization. This implies that both polarizations are complementary to each other and their combination can be useful for more accurate biomass estimation.

The correlations in multi-temporal data (2007-2010) are being compared to the mono-temporal data in the year 2010 when the field data were collected. As can be seen from Table 1 and Table 2, the correlations in single images are weaker compare to the multi-temporal approach in both HH and HV polarizations.

The average images of the whole time span data (2007-2010) were then used for developing biomass model. For scene 518-560, the correlation for HH and HV polarization is highly significant with r = 0.45 and r = 0.44, respectively. For scene 519-560, the correlation is also highly significant with r value for the HH polarization (r = 0.39) is weaker compare to the HV polarization (r = 0.43).

Table 2: Pearson's product moment correlation between AGB and backscatter coefficient for scene 519-560

		Scene 519-560					
		All classes		Sal		TMH	
		HH	HV	HH	HV	HH	HV
17 Aug 2007	r	0.38361	0.421073	0.46753	0.44146	0.34598	0.40816
	p-value	3.239e-05	4.187e-06	0.00918	0.146	0.00178	0.000188
2 Oct 2007	r	0.3877	0.46273	0.38287	0.53833	0.36142	0.44396
	p-value	2.616e-05	3.165e-07	0.03677	0.00214	0.0010	4.161e-05
2007	r	0.3998	0.4530	0.4427	0.5285	0.36635	0.4332
	p-value	1.378e-05	5.943e-07	0.01429	0.00267	0.000898	6.644e-05
19 May 2008	r	0.4073	0.43550	0.30775	0.33458	0.42097	0.46189
	p-value	9.112e-06	1.779-06	0.09803	0.07073	0.00011	1.828e-05
2008	r	0.4073	0.43550	0.30775	0.33458	0.42097	0.46189
	p-value	9.112e-06	1.779-06	0.09803	0.07073	0.00011	1.828e-05
22 Aug 2009	r	0.3023	0.3546	0.13033	0.26664	0.35203	0.36385
	p-value	0.0012	0.0001	0.4924	0.1544	0.0014	0.00098
2009	r	0.3023	0.3546	0.13033	0.26664	0.35203	0.36385
	p-value	0.0012	0.0001	0.4924	0.1544	0.0014	0.00098
10 Jul 2010	r	0.2731	0.37501	0.19887	0.08777	0.33932	0.41322
	p-value	0.0037	5.007e-05	0.2921	0.6447	0.002219	0.000153
25 Aug 2010	r	0.3569	0.41876	0.16413	0.34811	0.39610	0.43846
	p-value	0.0001	4.783e-06	0.3861	0.5941	0.00030	5.307e-05
2010	r	0.3362	0.4158	0.02043	0.24932	0.3918	0.44344
	p-value	0.0003	5.648e-06	0.9147	0.184	0.00035	4.259e-05
2007 - 2010	r	0.3946	0.4320				
	p-value	1.819e-05	2.19e-06				

Non-linier biomass regression model for HH and HV polarization are shown in Figure 3a and Figure 3b, respectively. As it can be seen from the graphic, the model accuracy is limit by the saturation level in around 100-150 t/ha. The saturation point is the value of AGB after which an increase in AGB cannot be observed as an increase in the radar backscatter. Above this limit, the estimation of biomass is not accurate enough, however it can be used to map the spatial distribution of high biomass. The best-fit model for HH and HV polarization are:

$$\sigma° = a + b*\ln(AGB) + c*\ln(x)^2 \quad (2)$$

where σ° is the radar backscatter coefficient, AGB is the above ground biomass calculated from the field forest inventory data, and a,b,c are the variables which are different for each polarization (see Table 3).

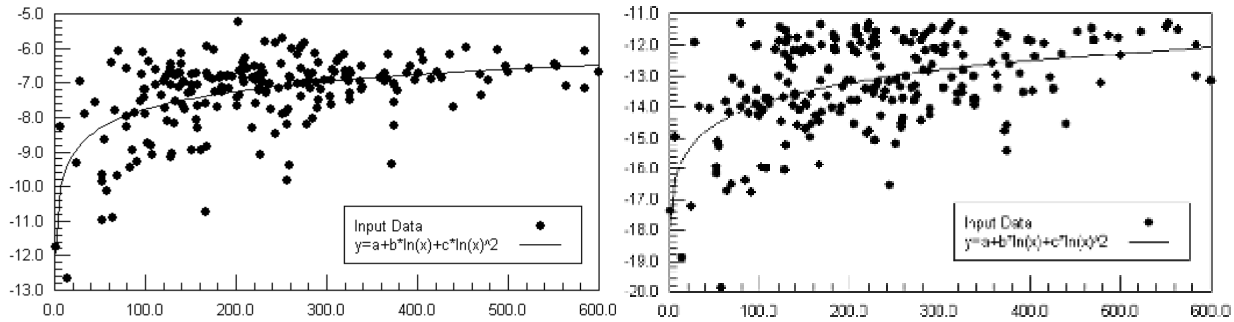

(a) (b)

Figure 3: The best-fit biomass model for (a) HH polarization; (b) HV polarization

The r^2 value shows that the regression line is not perfectly fit the data. The relatively low value is probably due to the complex structure of the forest and topographic factors in the study area. The terrain correction method may not be good enough to remove the effects of topography or slope in the images, resulting in poor relationships between AGB and radar backscatter. Other factors that may affect the AGB estimation performance, such as atmospheric conditions, mixed pixels, insufficient sample data, geometric registration errors, suitable extracted remote sensing variables, and the selected algorithms (Lu, 2006).

Table 3: Coefficients for radar biomass regression models

Polarization	a	b	c	r^2
HH	-11.905	1.029	-2.8E-02	0.296
HV	-17.875	0.737	2.672	0.249

Figure 4 shows the biomass map of Western Tiger Landscape Nepal in 2010 which was derived from the biomass model of multi-temporal HV polarization. As expected, the overall trends show the spatial distribution of high biomass value in the forest area (gradation of green color) and low biomass in the non-forest area (gradation of red color).

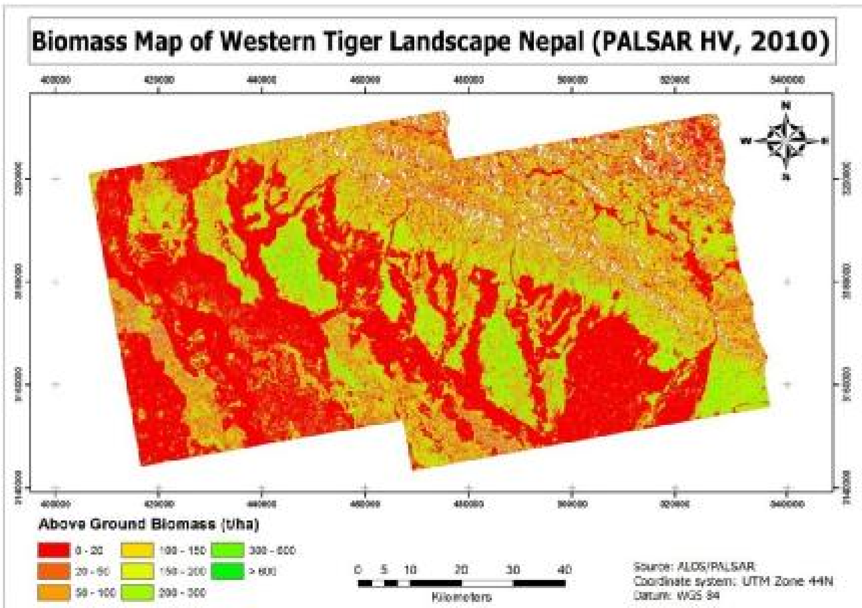

Figure 4: Biomass map of the Western Tiger Landscape Nepal in 2010

CONCLUSIONS & RECOMMENDATIONS

In the areas where forest stand structures, terrain or topographic characteristics, and environmental conditions are complex, biomass estimation is a challenging task. While the AGB estimation using traditional field measurement techniques have constraints in providing the spatial distribution of biomass in large areas and difficult terrain, remote sensing techniques greatly increase the usefulness in such conditions. However, the signals from remote-sensing instruments tend to saturate at high biomass level, no exception with the radar backscatter even though much higher biomass level can be achieved compared to the optical remote sensing. This study shows saturation level of L-band ALOS/PALSAR at 100-150 tons/ha.

In general, the multi-temporal data provides a stronger correlation with the AGB calculated from the field data compare to the mono-temporal approach. The multi-temporal approach compensates variable and extreme climatic conditions of a single radar image which may affect the radar signal interaction with the forest structure variables (Englhart et al., 2011).

The biomass model successfully produced a biomass map that shows the spatial distribution of forest biomass in a wide range of biomass values. However, the accuracy was relatively low and may not be in agreement with many other researches. Complex terrain and forest structures in the study area may lead to a poor correlation between radar backscatter and AGB calculated from the field inventory. More efforts should be made to remove the terrain effects with an appropriate model-based slope correction. Investigations using radar backscatter derived variables such as texture and combination of dual polarizations ratios may improve the accuracy of the model. Integration with other remote sensing data such as LiDAR (Light Detection and Ranging) and very high resolution images may be able to overcome the limitations of each data and complement each other.

ACKNOWLEDGEMENTS

This research has been financially supported through the JAXA Mini Project 2011-2012. The ALOS/PALSAR data were provided in the frame of the project.

REFERENCES:

References from Journals:

Asner, G.P., 2009. Tropical forest carbon assessment: integrating satellite and airborne mapping approaches. Environmental Research Letters 4 (3), 11pp.

Englhart, S., Keuck, V., Siegert, F., 2011. Aboveground biomass retrieval in tropical forest – The potential of combined X- and L-band SAR data use. Remote Sensing of Environment 115, pp. 1260-1271.

Gibbs, H.K., Brown, S., Niles, J.O., Foley, J.A., 2007. Monitoring and estimating tropical forest carbon stocks: making REDD a reality. Environmental Research Letters 2 (4), 13pp.

Koch, B., 2010. Status and future of laser scanning, synthetic aperture radar and hyperspectral remote sensing data for forest biomass assessment. ISPRS Journal of Photogrammetry and Remote Sensing 65, pp. 581-590.

Lu, D.S., 2006. The potential and challenge of remote sensing-based biomass estimation. International Journal of Remote Sensing, 27 (7), pp. 1297-1328.

Lucas, R., Armston, J., Fairfax, R., Fensham, R., Accad, A., Carreiras, J., Kelley, J., Bunting, J., Clewley, D., Bray, S., Metcalfe, D., Dwyer, J., Bowen, M., Eyre, T., Laidlaw, M., Shimada, M., 2010. IEEE Journal of Selected Topics in Applied Earth Observations and Remote Sensing 3(4), pp. 576-593.

Mitchard, E.T.A., Saatchi, S.S., Lewis, S.L., Feldpausch, T.R., Woodhouse, I.H., Sonke, B., Rowland, C., Meir, P., 2011. Measuring biomass changes due to woody encroachment and deforestation/degradation in a forest-savanna boundary region of central Africa using multi-temporal L-band radar backscatter. Remote Sensing of Environment 115, pp. 2861-2873.

Morel, A.C., Saatchi, S.S., Malhi, Y., Berry, N.J., Banin, L., Burslem, D., Nilus, R., Ong, R.C., 2011. Estimating aboveground biomass in forest and oil palm plantation in Sabah, Malaysia Borneo using ALOS PALSAR data. Forest Ecology and Management 262, pp. 1786-1798.

Patenaude, G., Milne, R., Dawson, T.P., 2005. Synthesis of remote sensing approaches for forest carbon estimation: reporting to the Kyoto Protocol. Environmental Science & Policy 8, pp. 161-178.

Sarker, M.L.R., Nichol, J., Ahmad, B., Busu, I., Rahman, A.A., 2012. Potential of texture measurements of two-date dual polarization PALSAR data for the improvement of forest biomass estimation. ISPRS Journal of Photogrammetry and Remote Sensing 69, pp. 146-166.

Shimada, M., Isoguchi, O., Tadono, T., & Isono, K., 2009. PALSAR radiometric calibration and geometric calibration. IEEE Transactions on Geoscience and Remote Sensing 47, pp. 3915-3932.

Sun, G., Ranson, K.J., Guo, Z., Zhang, Z., Montesano, P., Kimes, D., 2011. Forest biomass mapping from lidar and radar synergies. Remote Sensing of Environment 115, pp. 2906-2916.

Tian, X., Su, Z., Chen, E., Li, Z., van der Tol, C., Guo, J., He, Q., 2012. Estimation of forest above-ground biomass using multi-parameter remote sensing data over cold and arid area. International Journal of Applied Earth Observation and Geoinformation 14, pp. 160-168.

References from Other Literature:

Gurung, M B., and Kokh, M., 2011. Forest carbon accounting study report: Baseline, optimum sequestration potential and economics of REDD+ in the Terai Arc Landscape of Nepal. WWF Nepal.

GTOS (Global Terrestrial Observing System), 2009. Assessment of the status of the development of the standards for the terrestrial essential climate variables: Biomass. Report FAO.